Synthesis of heteroleptic iron(II) 2-pyridylmethylamides and 2-pyridylmethylideneamines *via* the reaction of [(thf)Fe{N(SiMe$_3$)$_2$}$_2$Cl] with (2-pyridylmethyl)(trialkylsilyl)amines†

Astrid Malassa, Nicole Herzer, Helmar Görls and Matthias Westerhausen*

Received 18th December 2009, Accepted 13th April 2010
First published as an Advance Article on the web 6th May 2010
DOI: 10.1039/b926723a

The deprotonation of (2-pyridylmethyl)(triorganylsilyl)amines of the type Py-CH$_2$-N(H)-SiR$_3$ with SiR$_3$ = SiMe$_2$*t*Bu (**1a**), SiMe$_2$(CMe$_2$*i*Pr) (**1b**), Si*i*Pr$_3$ (**1c**) and SiPh$_3$ (**1d**) with (thf)Fe[N(SiMe$_3$)$_2$]$_2$Cl in THF is accompanied by redox reactions and leads to the formation of iron(II) compounds. The products with lower solubility precipitated first and are the pale yellow and paramagnetic complexes chloro-(2-pyridylmethyl)(triorganylsilyl)amido iron(II) [SiR$_3$ = SiMe$_2$*t*Bu (**2a**), SiMe$_2$(CMe$_2$*i*Pr) (**2b**), Si*i*Pr$_3$ (**2c**), and SiPh$_3$ (**2d**)]. These complexes crystallized dimeric with Fe$_2$N$_2$ rings with different Fe–N bond lengths (average values of 211.1 and 203.2 pm). The Fe–Cl distances vary around an average value of 225.6 pm. Another isolated product consists of orange to blue crystals of dichloro-(2-pyridylmethylidene)(triorganylsilyl)amino iron(II) [SiR$_3$ = SiMe$_2$*t*Bu (**3a**), SiMe$_2$(CMe$_2$*i*Pr) (**3b**), Si*i*Pr$_3$ (**3c**), and SiPh$_3$ (**3d**)] which are obtained from very concentrated reaction solutions. These (2-pyridylmethylidene)(triorganylsilyl)amino ligands (imines) act as bidentate bases at FeCl$_2$ with average Fe–N and Fe–Cl bond lengths of 211.8 and 223.5 pm, respectively. The metallation of the (2-pyridylmethyl)(triorganylsilyl)amines with dimeric Fe[N(SiMe$_3$)$_2$]$_2$ yields homoleptic iron(II) bis[(2-pyridylmethyl)(triorganylsilyl)amides] (**4**) with distorted tetrahedrally coordinated iron centers. Metathesis reactions of FeCl$_3$ with lithium (2-pyridylmethyl)(triorganylsilyl)amide as well as employing a mixture of Fe[N(SiMe$_3$)$_2$]$_2$ and FeCl$_3$ with (2-pyridylmethyl)(triorganylsilyl)amine give similar results and the formation of chloro-(2-pyridylmethyl)(triorganylsilyl)amido iron(II) (**2**) and dichloro-(2-pyridylmethylidene)(triorganylsilyl)amino iron(II) (**3**) are observed.

Introduction

The amides of the late transition metals have attracted considerable interest due to their application in chemical processes[1] and as models in biomimetic studies.[2] Oxidation reactions of biological processes often are catalyzed by iron enzymes such as lipoxygenases and methane monooxygenases.[3] These non-heme iron enzymes are able to oxidize unsaturated fatty acids or methane with oxygen after activation of the appropriate C–H bonds. The catalytic activity led to a large interest in compounds with iron–nitrogen bonds and in many biomimetic model complexes, substituted pyridine ligands are employed to mimic the reactivity of these iron enzymes.[4] Iron complexes are known to oxidize hydrocarbons whereby the most reactive compounds contain pyridylmethylamine fragments in the coordination sphere.[5-8] Recently, Ostermeier *et al.*[9] oxidized 1,4-bis(2-pyridylmethyl)piperazine in the coordination sphere of FeCl$_3$ (eqn (1)).

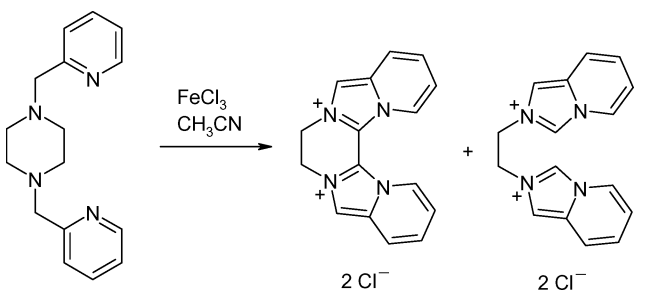

(1)

Wieghardt and coworkers[10] reacted the imine (L^{ox2})^0 with the transition metal salts M^{II}Cl$_2$ of Cr, Mn, Fe, Co, Ni, and Zn and reduced these complexes with sodium in 1,2-dimethoxyethane, (L^{ox2})^0 being the imine [2-Py-CH=N–C$_6$H$_3$*i*Pr$_2$]. This reduction gave the complexes [M^{II}(L^{ox1})$_2$] (see Scheme 1). Cyclovoltammetric investigations showed that this redox reaction is reversible. The oxidation of these complexes with [Cp$_2$Fe^{III}]$^+$ in THF yielded [(thf)M^{II}(L^{ox1})(L^{ox2})]$^+$ (M = Cr, Mn, Fe, Co), [Zn^{II}(L^{ox1})(L^{ox2})]$^+$, and [Ni(L^{ox2})$_2$]$^+$, respectively. In [Fe^{II}(L^{ox1})$_2$] average Fe–N bond lengths of 198.5 and 204.5 pm were observed to the amide and the pyridyl bases. In [(thf)Fe^{II}(L^{ox1})(L^{ox2})]$^+$ the Fe–N distances of 198.9 and 200.4 pm are very much alike (Fe–O 206.0 pm).[10]

The radical anion (L^{ox1})$^-$ has already been observed earlier by van Koten and coworkers[11] as alkylzinc adduct [RZn(L^{ox1})]. In the solid state this zinc complex crystallizes as a dimer,

Institut für Anorganische und Analytische Chemie, Friedrich-Schiller-Universität Jena, August-Bebel-Str. 2, D-07743, Jena, Germany. E-mail: m.we@uni-jena.de; Fax: +49 3641 948102

† CCDC reference numbers 676619–676626 and 736365–736366. For crystallographic data in CIF or other electronic format see DOI: 10.1039/b926723a

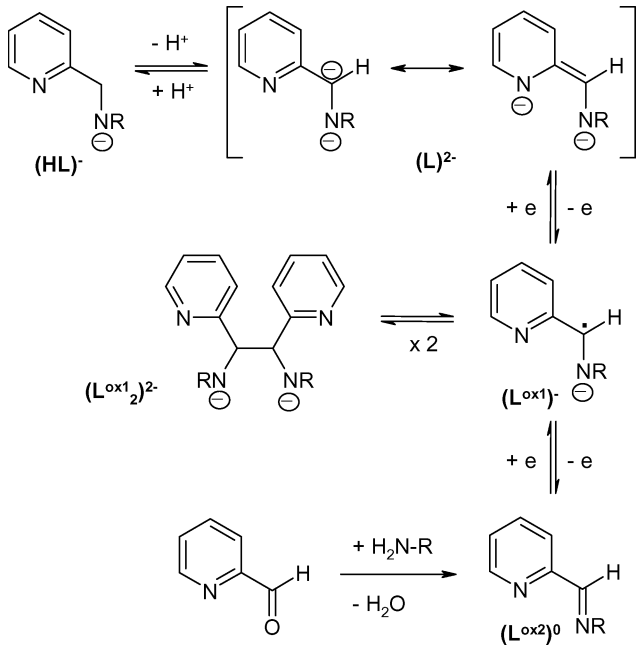

Scheme 1 Deprotonation/protonation and redox equilibria of 2-pyridylmethylamides.

namely bis(alkylzinc) 1,2-bis(2-pyridyl)-1,2-bis(alkylamido)-ethane [$(RZn)_2(L^{ox1}{}_2)$]. Bis(amide) complexes (containing the ligand $(L)^{2-}$) are only stable with very electropositive metals such as lithium[12] (as $[Li_2(L)]_8$) and magnesium[13] (as $[(thf)Mg(L)]_2$); the oxidation of $[Li_2(L)]_8$ with white phosphorous leads to the formation of $[Li_2(L^{ox1}{}_2)\cdot Li(HL)]$ and Li_3P_7.[14] In Scheme 1 the reaction diagram shows the interconversion of the bisamide $(L)^{2-}$ into $(L^{ox2})^0$ which can also be prepared from an aldehyde and a primary amine.

Metal-mediated oxidation of nitrogen-bound 2-pyridylmethyl groups is restricted to less electropositive metals. Thus, zinc complexes are able to initiate an oxidative C–C coupling reaction at elevated temperatures according to eqn (2).[13,15] In course of this oxidation process of (2-pyridylmethyl)(trialkylsilyl)amides of zinc (**A**) in the presence of dialkylzinc, zinc metal precipitates and di(methylzinc) 1,2-di(2-pyridyl)-1,2-bis(trialkylsilylamido)ethane (**B**) forms. Nobler metals such as tin(II) afford less drastic reaction conditions in order to enable this oxidative C–C coupling reaction. In the presence of air, 2-pyridylmethylamine can be oxidized by cobalt(II) yielding 2,3,5,6-tetra(2-pyridyl)pyrazine.[16,17]

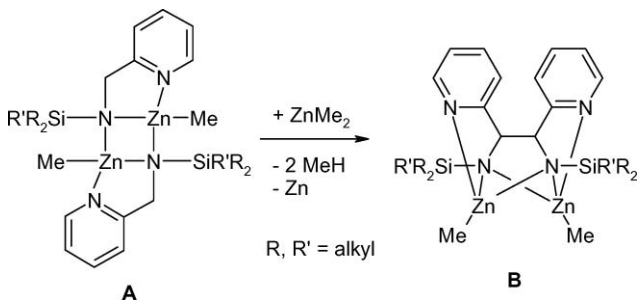

(2)

Iron(II) chloride complexes react with air as shown in eqn (3) *via* insertion of oxygen between the iron atoms of **C** raising the oxidation state from iron(II) to iron(III) in **D** without oxidation of the coordinated bis(2-pyridylmethyl)amine molecules.[18] Furthermore, various 2-pyridylmethylamine complexes of iron(II)[19-21] and iron(III)[21] were prepared and structurally investigated. From these amine complexes of iron halides, amide formation and liberation of HX was not observed.

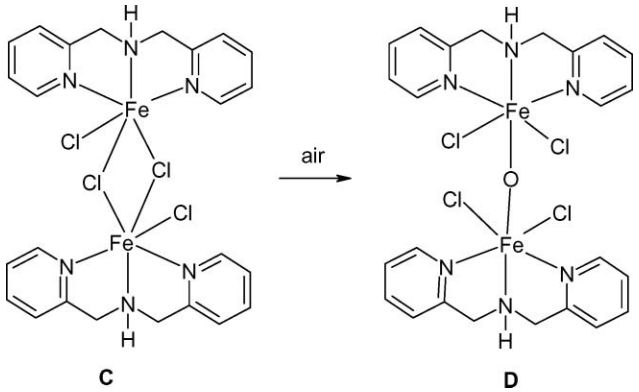

(3)

In contrast to these amine adducts of iron, dialkylamides of the late transition metals Fe, Co, Ni, and Cu are not stable because amides act as a two-electron σ-donor and as a two-electron π-donor which is only advantageous for electron-poor early transition metals.[22-24] A trialkylsilyl substituent at nitrogen reduces the charge at the amide unit *via* backdonation from the p_z(N) lone pair into a σ*(Si–C) bond and therefore, the trialkylsilyl-substituted amides of iron are well-known.[25,26]

On the one hand, these investigations showed that the bis(trimethylsilyl)amido group reacts as a metallating functionality in contrast to the chloride anion. On the other hand, the presence of chloro ligands allowed the synthesis of heteroleptic amido iron(II) chlorides which can be modified thereafter. In order to investigate oxidative C–C coupling reactions similar to Scheme 1, iron(III) compounds were reacted with (2-pyridylmethyl)(trialkylsilyl)amines. However, in $Fe[N(SiMe_3)_2]_3$[27] the metal center is shielded quite effectively by three bulky bis(trimethylsilyl)amido ligands. Therefore, $(thf)Fe[N(SiMe_3)_2]_2Cl$,[28,29] a mixture of $FeCl_3$ and $[Fe\{N(SiMe_3)_2\}_2]_2$, and the use of $FeCl_3$ after lithiation of the amine were employed for these investigations regarding the influence of the bulkiness of the *N*-bound trialkylsilyl groups of 2-pyridylmethylamine on the reactivity.

Results and discussion

(2-Pyridylmethyl)(trialkylsilyl)amines of the type Py-CH_2-N(H)-SiR_3 (SiR_3 = $SiMe_2tBu$ (**1a**),[15] $SiMe_2(CMe_2iPr)$ (**1b**), $SiiPr_3$ (**1c**),[13] and $SiPh_3$ (**1d**)) were deprotonated with $(thf)Fe[N(SiMe_3)_2]_2Cl$ and metallated [leading to the amide ligands $(HL)^-$ of **2**] or oxidized [yielding imine ligands $(L^{ox2})^0$ of **3**] as shown in eqn (4). The pale yellow complexes chloro-(2-pyridylmethyl)-(trialkylsilyl)amidoiron(II) [SiR_3 = $SiMe_2tBu$ (**2a**), $SiMe_2(CMe_2iPr)$ (**2b**), $SiiPr_3$ (**2c**), and $SiPh_3$ (**2d**)] precipitated with yields between 16% (**2c**) and 42% (**2a**). These compounds are paramagnetic with high-spin iron atoms which show an antiferromagnetic coupling.

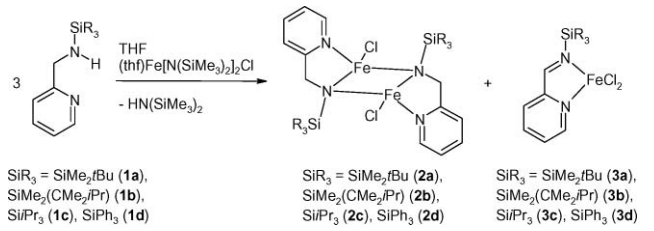

(4)

During this metallation reaction, the iron(III) atoms were reduced to iron(II), elemental iron was not observed. The expected coupling product 1,2-dipyridyl-1,2-bis(trialkylsilylamino)ethane was neither detected in the mass spectrometric investigations nor after common work-up procedures. In addition, the formation of tetrakis(trimethylsilyl)hydrazine could be excluded as well. However, the use of the silyl groups $SiMe_2tBu$, $SiMe_2(CMe_2iPr)$, $SiiPr_3$, and $SiPh_3$ led to the crystallization of red by-products which were identified as the (2-pyridylmethylidene)(triorganylsilyl)amine adducts of $FeCl_2$ (**3a**, **3b**, **3c** and **3d**).

(2-Pyridylmethyl)(*tert*-butyldimethylsilyl)amido groups stabilize iron(II). In contrast to the stability of $Fe[N(SiMe_3)_2]_3$ no derivatives of iron(III) were obtained for these 2-pyridylmethylamido ligands. Furthermore, the zinc(II) complexes were able to induce an oxidative C–C coupling of these ligands with formation of zinc metal as shown in eqn (2). Oxidative C–C coupling reactions of the (2-pyridylmethyl)(trialkylsilyl)amido moieties were neither observed from the redox reactions of the iron(III) complexes nor from the metathesis reactions of the iron(II) species. However, iron(III) was reduced to iron(II). In order to test the influence of the bis(trimethylsilyl)amido groups, the metathesis reaction of $FeCl_3$ with $LiN(SiR_3)CH_2Py$ was investigated. This reaction also led to a reduction of Fe^{3+} and iron(II) complexes **2a** and **2d** as well as **3b** and **3c** were isolated.

From a mixture of $[Fe\{N(SiMe_3)_2\}_2]_2$ and (2-pyridylmethyl)-(trialkylsilyl)amine the homoleptic complexes **4a** to **4d** were prepared (eqn (5)).[26] Addition of $FeCl_3$ (1 : 1 ratio of Fe^{2+} : Fe^{3+}) to this solution led to the formation of the imino complexes **3a** to **3d** and to the amido complexes **2a** to **2d** of iron(II) (eqn (5)). Besides compounds **2** and **3**, the well-known $(thf)_6Fe_4Cl_8$[30] was also found. However, no iron(III) compounds were observed in this reaction; iron(III) was reduced to iron(II) and the amine was oxidized to the imino ligand yielding complexes **3a** to **3d**.

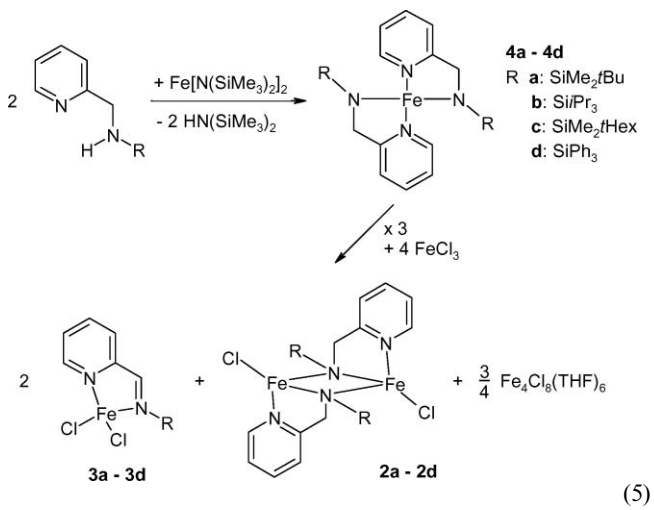

(5)

The intermediate of the reaction of homoleptic iron(II) bis[(2-pyridylmethyl)(trialkylsilyl)amides] **4** with $FeCl_3$ could be a mixed valent, dinuclear coordination compound **G** which contains iron(II) as well as iron(III) (eqn (6)). An additional chloro ligand ensures electro-neutrality. This intermediate could also resemble the intermediate in the other reaction sequences described in eqn (6).

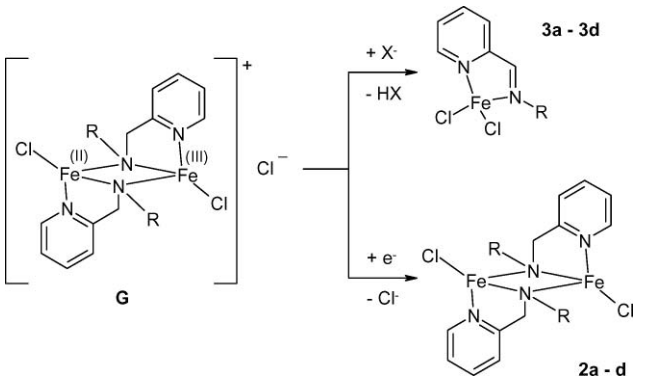

(6)

Deprotonation of the methylene moiety can be achieved by strong bases. Lithiation and magnesiation of 2-pyridylmethylamides lead to dianions of the type $(L)^{2-}$[12,13] which can be characterized by X-ray crystallography because these metal cations are non-redox active. A similar metallation reaction of $[Fe\{N(SiMe_3)_2\}_2]_2$ and $(thf)Fe[N(SiMe_3)_2]_2Cl$ or of iron(II) bis[(2-pyridylmethyl)(trialkylsilyl)amides] **4** in the presence of iron(III) would initiate an immediate redox reaction yielding the imine complexes **3a** to **3d**.

Molecular structures

The molecular structure of (2-pyridylmethyl)(triphenylsilyl)amine (**1d**) is displayed in Fig. 1. The hydrogen atom H1 at N1 was refined isotropically and a N1–H1 bond length of 84(2) pm was observed. This N1 atom lies in a nearly planar environment with an angle sum of 351°. The N1–Si bond length of 171.4(2) pm is rather short. This shortening is a consequence of a larger s-orbital participation in the amine **1d** due to a sp^2 hybridized N1 atom. The N1–C1 distance of 145.9(3) pm resembles a characteristic single bond.

The molecular structures of **2a** to **2d** are very similar (Table 1) and therefore, only the structures of (2-pyridylmethyl)(*tert*-butyldimethylsilyl)amido iron(II) chloride (**2a**) and (2-pyridylmethyl)(triphenylsilyl)amido iron(II) chloride (**2d**) are shown in Fig. 2 and 3, respectively, as representative examples. The central four-membered Fe_2N_2 rings of **2a**, **2b**, and **2d** contain crystallographic inversion centers and consequently, these rings are strictly planar and the symmetry-equivalent groups are on different sides of the Fe_2N_2 plane (*trans*-annular *trans* arrangement). The iron and amide nitrogen atoms show distorted tetrahedral environments. However, due to ring strain the endocyclic bond angles at iron display very small values (N1–Fe–N2 81.8(1)°, N2–Fe–N2A 95.9(1)°). The Fe–N2 and Fe–N2A bond lengths differ significantly. The Fe–N2 bond lengths are larger than the Fe–N2A values because the Fe–N2 values resemble bonds with ring strain due to annelated four- and five-membered rings whereas Fe–N2A bonds are only a bond of a four-membered cycle.

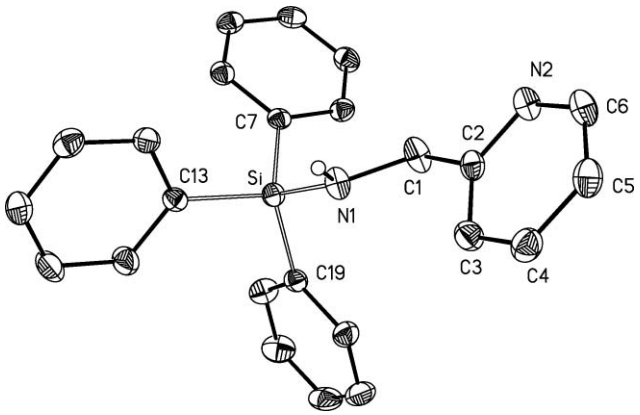

Fig. 1 Molecular structure and numbering scheme of (2-pyridylmethyl)(triphenylsilyl)amine (**1d**). The ellipsoids represent a probability of 40%. Hydrogen atoms with the exception of the NH moiety are neglected for clarity reasons. Selected bond lengths (pm): Si–N1 171.4(2), Si–C7 188.3(2), Si–C13 186.8(2), Si–C19 187.0(2), N1–C1 145.9(3), N1–H1 84(2), C1–C2 150.9(3), N2–C2 133.8(3), N2–C6 134.2(3); selected angles (°): Si–N1–C1 125.0(1), C1–N1–H1 111(2), Si–N1–H1 115(2), N1–C1–C2 112.3(2).

Table 1 Selected structural data of heteroleptic [ClFe-N(SiR_2R')-(CH_2Py)]$_2$ (**2a–d**)

	2a	**2b**	**2c**	**2d**
R	Me	Me	*i*Pr	Ph
R′	*t*Bu	CMe_2*i*Pr	*i*Pr	Ph
Fe–Cl	225.27(8)	226.25(6)	225.3(1)	225.7(1)
Fe–N2	211.1(2)	211.1(2)	210.9(2)	211.4(3)
Fe–N2A	201.8(2)	202.0(2)	205.0(2)	203.9(3)
Fe–N1	208.4(2)	208.2(2)	207.8(2)	208.7(3)
Si–N2	175.4(2)	176.0(2)	176.6(2)	174.1(3)
N2–C6	149.0(3)	148.7(2)	148.9(4)	149.8(4)
C5–C6	150.9(4)	150.6(3)	151.5(4)	150.3(5)
Fe···FeA	272.98(8)	275.20(6)	275.43(7)	278.1(1)
Cl–Fe–N1	102.09(7)	101.84(5)	101.05(7)	101.2(1)
Cl–Fe–N2	128.61(6)	134.06(5)	131.55(7)	135.40(9)
Cl–Fe–N2A	117.03(6)	113.32(5)	115.53(7)	113.34(9)
N1–Fe–N2	82.01(8)	81.91(7)	82.44(9)	81.8(1)
N1–Fe–N2A	127.91(9)	130.09(7)	128.90(9)	130.5(1)
N2–Fe–N2a	97.24(7)	96.49(7)	96.92(9)	95.9(1)
N2–C6–C5	113.5(2)	113.8(2)	114.8(2)	113.7(3)

Increasing bulkiness of the trialkylsilyl groups leads to enhanced non-bonding transannular Fe···FeA contacts.

Furthermore, the N2–C6 distances of the dimeric (2-pyridylmethyl)(trialkylsilyl)amido iron(II) chlorides with an average value of 149.1 pm are significantly larger than the corresponding value of **1d** (145.9(3) pm). The Si–N2 bond lengths of 175.5 pm (av. value) are also larger due to the coordination number of four which suggests a sp^3 hybridization of N2 and consequently a reduced s-orbital participation in the bonds.

Selected structural parameters of the monomeric (2-pyridylmethylidene)(trialkylsilyl)amine complexes of $FeCl_2$ (**3a** to **3c**) as well as of dimeric **3d** are summarized in Table 2. As a representative example of a monomeric derivative **3a** is shown in Fig. 4. The iron atoms are in a distorted tetrahedral environment with average Fe–Cl distances of 223.45 pm which is a slightly smaller value than observed for **2**. The Fe–N2 bond lengths are slightly larger than in **2** due to the reduced electrostatic attraction in **3**.

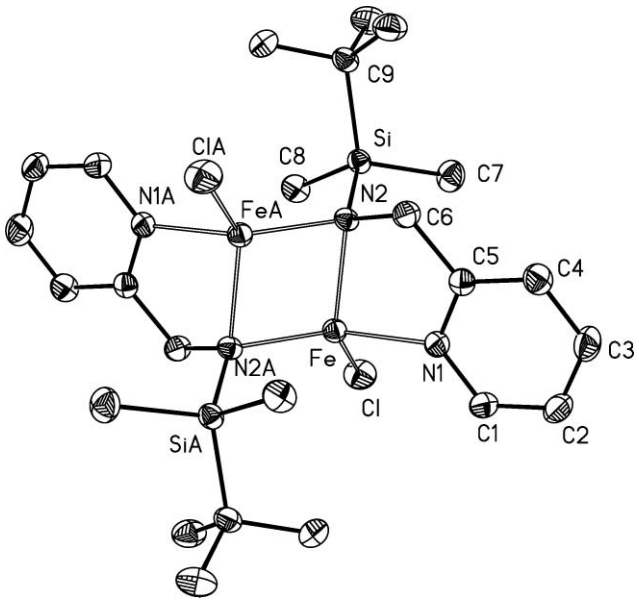

Fig. 2 Molecular structure and numbering scheme of chloro-(2-pyridylmethyl)(*tert*-butyldimethylsilyl)amidoiron(II) (**2a**). The ellipsoids represent a probability of 40%. H atoms are not shown due to clarity reasons. Symmetry-related atoms ($-x + 2, -y + 1, -z$) are marked with "A". Selected structural data are given in Table 1.

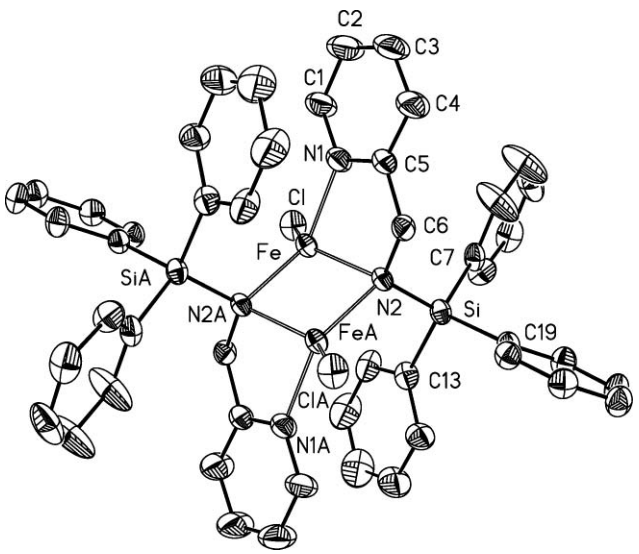

Fig. 3 Molecular structure and numbering scheme of chloro-(2-pyridylmethyl)(triphenylsilyl)amidoiron(II) (**2d**). The ellipsoids represent a probability of 40%. H atoms are omitted for clarity reasons. Symmetry-related atoms ($-x + 3/2, -y + 1/2, -z$) are marked with "A". Selected structural data are summarized in Table 1.

The imino ligand contains a planar coordinated N2 atom with a N2=C6 double bond (av. value 127.6 pm). However, there is nearly no interaction with the π-system of the pyridyl unit; the slight shortening of this bond compared to **2** results from an enhanced s-orbital contribution. Surprisingly, the N2–Si bond lengths are rather large and show an average value of 179.9 pm (compare with **2**: av. N2–Si 175.5 pm). This fact can be explained by reduced electrostatic attraction due to the lack of anionic charge on the ligand which also reduces the negative hyperconjugation from the

Table 2 Selected structural data for the imine complexes **3** of the type (2-Py-CH=N-SiR_2R′)FeCl_2. Complex **3d** precipitates as a dimer whereas **3a–3c** crystallize monomeric

	3	**3b**	**3c**	**3d**
R	Me	Me	*i*Pr	Ph
R′	*t*Bu	CMe_2*i*Pr	*i*Pr	Ph
Fe–Cl1	223.12(9)	223.63(9)	224.19(7)	237.27(8)
Fe–Cl2	223.63(9)	223.37(9)	222.78(7)	226.40(8)
Fe–Cl1A	—	—	—	253.53(7)
Fe–N2	212.0(2)	213.9(2)	213.0(2)	221.7(2)
Fe–N1	210.9(2)	210.0(2)	210.9(2)	213.0(2)
Si–N2	178.8(3)	180.0(2)	180.9(2)	178.9(2)
N2–C6	127.6(4)	127.8(4)	127.5(3)	127.6(4)
C5–C6	146.7(4)	147.7(4)	147.8(3)	147.2(4)
N2–Fe–N1	78.82(9)	78.91(9)	79.227	77.68(8)
N1–Fe–Cl1	111.62(7)	114.56(7)	105.54(5)	106.91(7)
Cl1–Fe–Cl2	121.67(4)	119.13(4)	122.09(3)	136.15(3)
Cl2–Fe–N2	113.85(7)	124.4(2)	113.98(5)	91.77(6)
Si–N2–C6	123.4(2)	121.4(2)	120.2(2)	118.9(2)
C6–N2–Fe	112.3(2)	111.8(2)	111.4(1)	110.5(2)
Fe–N2–Si	124.1(1)	126.4(1)	128.41(9)	130.0(1)
N2–C6–C5	120.8(3)	120.7(3)	121.6(2)	121.9(2)

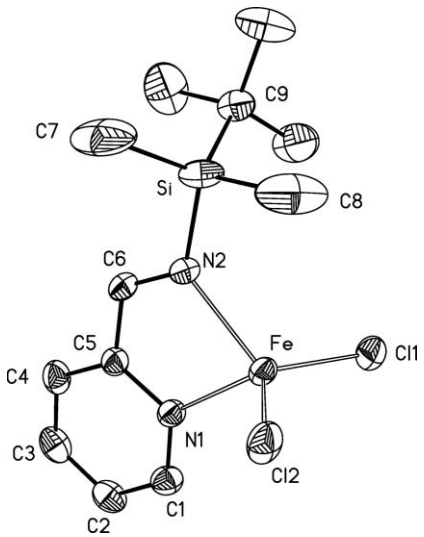

Fig. 4 Molecular structure and numbering scheme of dichloro-(2-pyridylmethylidene)(*tert*-butyldimethylsilyl)aminoiron(II) (**3a**). The ellipsoids represent a probability of 40%. H atoms are neglected for clarity reasons. Selected structural data are summarized in Table 2.

nitrogen lone pair into the σ*(Si–C) bond. The larger N2–C6–C5 angles in **3** also lead to larger N1–Fe–N2 angles.

The molecular structure and numbering scheme of dimeric dichloro-(2-pyridylmethylidene)(triphenylsilyl)aminoiron(II) (**3d**) is shown in Fig. 5. The dimeric nature of this complex nearly does not affect the imino ligand. However, the coordination sphere at the penta-coordinate iron atom differs strongly from those of the monomeric derivatives. In the trigonal bipyramidal environment of iron the atoms N2 and Cl1A are arranged in axial positions (N2–Fe–Cl1A 170.98(6)°) whereas N1, Cl1 and Cl2 form the trigonal plane. Due to the *trans* arrangement of the atoms N2 and Cl1A and due to the high spin state of the iron center the Fe–N2 as well as Fe–Cl1A bonds are elongated. A detailed discussion of a bonding situation in comparable iron complexes regarding the trigonal bipyramidal as well as the square pyramidal coordination sphere at iron can be found elsewhere.[32]

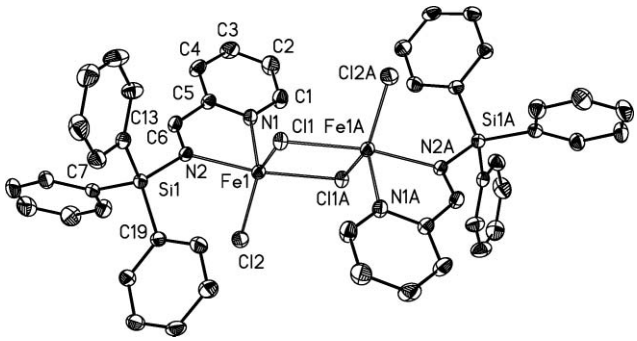

Fig. 5 Molecular structure and numbering scheme of dichloro-(2-pyridylmethylidene)(triphenylsilyl)aminoiron(II) (**3d**). Symmetry-related atoms (−*x* + 2, −*y* + 1, −*z* + 1) are marked with an apostrophe. The ellipsoids represent a probability of 40%. H atoms are neglected for clarity reasons. Selected structural data are summarized in Table 2. Coordination sphere of Fe1 (°): N1–Fe1–N2 77.68(8), N1–Fe1–Cl1 106.91(7), N1–Fe1–Cl2 116.57(7), N1–Fe1–Cl1A 94.20(6), N2–Fe1–Cl1 92.06(6), N2–Fe1–Cl2 91.77(6), N2–Fe1–Cl1A 170.98(6), Cl1–Fe1–Cl2 136.15(3), Cl1–Fe1–Cl1A 86.53(2), Cl2–Fe1–Cl1A 95.42(3).

Table 3 Comparison of selected structural data of iron(II) bis[2-pyridylmethyl)(*tert*-butyldimethylsilyl)amide] **4a**[25] and iron(II) bis[2-pyridylmethyl)(triphenylsilyl)amide] **4d**

	4a (R = $SiMe_2$*t*Bu)	**4d** (R = $SiPh_3$)
Fe1–N1	212.3(2)	211.2(2)
Fe1–N2	196.1(2)	196.7(2)
Si1–N2	170.3(2)	168.8(2)
N2–C6	145.3(2)	145.6(3)
C6–C5	150.4(3)	150.7(4)
C5–N1	133.8(2)	134.7(3)
Si–C7	188.7(2)	189.0(3)
N2–Fe1–N1	82.21(6)	81.86(9)
N2A–Fe1–N1	111.79(6)	122.30(9)
N2–Fe1–N2A	155.5(1)	143.4(1)
N1–Fe–N1A	112.54(8)	102.7(1)

It is remarkable that the imino complexes **3a–c** are monomeric whereas **3d** crystallizes as a dimer. This fact shows that the triphenylsilyl group induces smaller steric strain than the trialkylsilyl groups which allows a larger coordination number at the iron center. Similar structural parameters of the imino ligands in **3a–d** exclude strong electronic effects.

Molecular structure and numbering scheme of **4d** is shown in Fig. 6. The iron atom is in a distorted tetrahedral environment. Selected structural parameters of this complex are compared with those of **4a** in order to detect the influence of steric hindrance (Table 3).[25] The bond lengths show nearly no dependency whether $SiMe_2$*t*Bu or $SiPh_3$ groups are attached to N2. The endocyclic N1–Fe–N2 also show very similar values. However, all endocyclic bond angles differ strongly because the triphenylsilyl substituents are less bulky than the *tert*-butyldimethylsilyl groups. This fact leads to a smaller N2–Fe–N2A angle whereas the N2A–Fe–N1 angle is widened by approximately 10°. These distortions allow a coplanar alignment of the pyridyl group and one of the silicon-bound phenyl substituents.

The aggregation degree strongly depends on the bulkiness of the *N*-bound substituent. Gibson *et al.*[31] already found monomeric

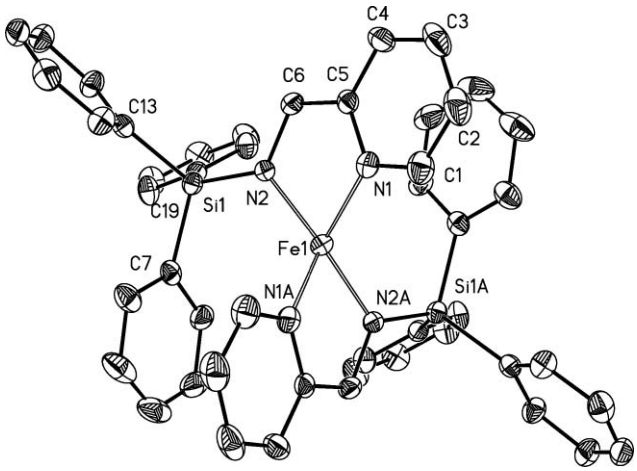

Fig. 6 Molecular structure and numbering scheme of iron(II) bis[(2-pyridylmethyl)(triphenylsilyl)amide] **4d**. Symmetry-related atoms ($-x + 1/2$, $-y + 1/2$, z) are marked with an "A". The ellipsoids represent a probability of 40%. Hydrogen atoms are not drawn for clarity reasons. Selected bond lengths (pm): Fe1–N1 211.2(2), Fe1–N2 196.7(2), Si1–N2 168.8(2), N1–C1 134.9(4), N1–C5 134.7(3), C1–C2 136.8(4), C2–C3 138.4(5), C3–C4 137.7(4), C4–C5 138.4(4), C5–C6 150.7(4). Angles (°): N1–Fe1–N2 81.86(9), N1–Fe1–N1A 102.7(1), N1–Fe1–N2A 122.30(9), N2–Fe1–N2A 143.4(1), Fe1–N2–Si1 122.9(1), Fe1–N2–C6 113.4(2), Si1–N2–C6 123.7(2).

complexes of the type $[Cl_2Fe(2\text{-Py}'\text{-CH=NR})]$ (Py′ = 6-methyl-2-pyridyl) for ligands with nitrogen-bound cyclo-dodecyl groups. Less bulky *n*-propyl and *ortho*-diisopropylphenyl substituents give dimeric molecules $[(2\text{-Py}'\text{-CH=NR})Fe(Cl)(\mu\text{-Cl})]_2$ with penta-coordinate iron atoms in distorted trigonal bipyramidal and square pyramidal environments, respectively. An enhanced coordination number of iron also leads to elongated Fe–N bonds.

Iron(III) has to be considered as a rather strong oxidation reagent. Therefore, the oxidation of ligands of the type $(L)^{2-}$ always led to the formation of imines $(L^{ox2})^0$ (see eqn (2)). Milder oxidation reagents such as zinc(II) and tin(II) allowed the observation and isolation of $(L^{ox1})^-$ and its dimer $(L^{ox1}{}_2)^{2-}$.

Conclusion

The iron(III) complex $(thf)Fe[N(SiMe_3)_2]_2Cl$ is a valuable starting material for the synthesis of pale yellow heteroleptic $[ClFeN(SiR_3)CH_2Py]_2$ (**2**) because the chloride anion acts as a spectator ligand and shows no tendency to interfere with the metallation reaction. The bis(trimethylsilyl)amide group, however, is an effective metallating functionality. During the metallation of (2-pyridylmethyl)(trialkylsilyl)amine (**1**), iron(III) is reduced to iron(II). In course of this redox reaction, red crystals of the (2-pyridylmethylidene)(trialkylsilyl)amine adducts of $FeCl_2$ (**3**) precipitate. These imino ligands form *via* an oxidation of the iron-bound (2-pyridylmethyl)(trialkylsilyl)amide substituents. A proposed reaction sequence which explains the formation of **2** and **3** is summarized in Scheme 2.

The compounds described here are not only accessible *via* the metallation reaction of (2-pyridylmethyl)(trialkylsilyl)amines with $(thf)Fe[N(SiMe_3)_2]_2Cl$, but metathesis reactions of $FeCl_2$ with an equimolar amount of lithium (2-pyridylmethyl)-(trialkylsilyl)amide also allow the preparation of **2**. In addition, the redox reaction of lithium (2-pyridylmethyl)(trialkylsilyl)amide with $FeCl_3$ yields the heteroleptic complexes **2a** to **2d** as well as **3a** to **3d**.

A comparison of the structures with terminally iron-bound 2-pyridylmethylideneamines 2-Py-CH=NR or their reduced forms is shown in Table 4. The CN bond varies from a double bond (average C=N 127.5 pm) for the L^{ox2} type ligand, the reduced $(L^{ox1})^-$ type with C–N values of 133.9 pm to a single bond for the 2-pyridylmethylamides (HL^- type) with C–N distances of 145.5 pm. Increasing negative charge on the nitrogen atoms leads to a shortening of the Fe–N bonds. In addition, a lengthening of the Fe–N bonds (which can either affect the bond to the imino or the pyridyl groups) is also observed for dimeric complexes with penta-coordinate metal atoms.

Experimental

General procedure

All manipulations were carried out in an argon atmosphere under anaerobic conditions. The compounds are moisture and air sensitive. Prior to use, all solvents were thoroughly dried and distilled in an argon atmosphere. $(thf)Fe\{N(SiMe_3)_2\}Cl$[28,29] and the (2-pyridylmethyl)(trialkylsilyl)amines of the type $Py\text{-}CH_2\text{-}N(H)\text{-}SiR_3$ with $SiR_3 = SiMe_2tBu$ (**1a**)[15] and $SiiPr_3$ (**1c**)[13] were prepared according to literature procedures.

(2-Pyridylmethyl)(1,1,2-trimethylpropyl-dimethylsilyl)amine (1b)

A 2.5 M *n*-BuLi solution in hexane (8.0 ml, 20 mmol) was dropped into a solution of 2.2 g of 2-aminomethylpyridine (20 mmol) in 10 ml of THF. Chloro-1,1,2-trimethylpropyl-dimethylsilane (3.6 g, 20 mmol) dissolved in 10 ml of THF was added dropwise to this mixture at −78 °C. Thereafter the solution was warmed to r.t. and stirred for an additional 20 h. Then all volatile materials were removed under reduced pressure and the residue was dissolved in 10 ml of pentane. After removal of insoluble lithium salts, the solvent was removed again. Distillation gave 4.45 g of a colorless oil of **1b** (17.8 mmol, 89%) with a boiling point of 100 °C at 10^{-3} mbar. ^1H NMR (C_6D_6, δ (ppm)): 0.05 (s, 6H, $SiCH_3$), 0.83 (s, 6H, $SiC(CH_3)_2$), 0.86 (d, 6H, $CH(CH_3)_2$), 1.22 (br, 1H, NH), 1.58 (hept, 1H, $CH(CH_3)_2$), 4.09 (2H, CH_2), 6.63 (dd, 1H, Pyr2), 7.01 (d, 1H, Pyr4), 7.12 (dd, 1H, Pyr3), 8.42 (d, 1H, Pyr1), $^3J(CH_3\text{-}CH) = 6.8$ Hz), $^3J(CH\text{-}CH_3) = 6.8$ Hz, $^3J_o(H2\text{-}H1/3) =$ 6 Hz and 5.9 Hz), $^3J_o(H3\text{-}H4) = 7.6$ Hz), $^3J_o(H3\text{-}H2/4) = 7.3$ Hz), $^3J_o(H1\text{-}H2) = 4.4$ Hz). $^{13}C\{^1H\}$ NMR (C_6D_6, δ (ppm)): 2.4 ($Si(CH_3)_2$), 18.9 ($SiC(CH_3)_2$), 21.1 ($SiC(CH_3)_2$), 24.7 ($CH(CH_3)_2$), 34.7 ($CH(CH_3)_2$), 48.7 (CH_2), 120.8 (Pyr4), 121.3 (Pyr2), 135.9 (Pyr3), 149.2 (Pyr1), 163.7 (Pyr5). MS (DEI, m/z): 249 ($M^+ - H$); 164 ($Pyr\text{-}CH_2\text{-}N\text{-}Si(CH_3)_2$). IR (pure, KBr, ν/cm^{-1}: 3374 vs, 3067 w, 2957 vs, 2865 vs, 1591 vs, 1570 s, 1468 vs, 1433 vs, 1404 vs, 1377 s, 1343 w, 1318 w, 1249 vs, 1197 w, 1124 vs, 1085 s, 1047 m, 994 m, 971 w, 873 s, 825 vs, 775 vs, 678 w, 659 m, 628 w, 603 w, 494 w.

(2-Pyridylmethyl)(triphenylsilyl)amine (1d)

2-Aminomethylpyridin (1.1 g, 10.2 mmol) was deprotonated in 10 ml of THF at −78 °C with 6.3 ml of a 1.6 M *n*-BuLi solution

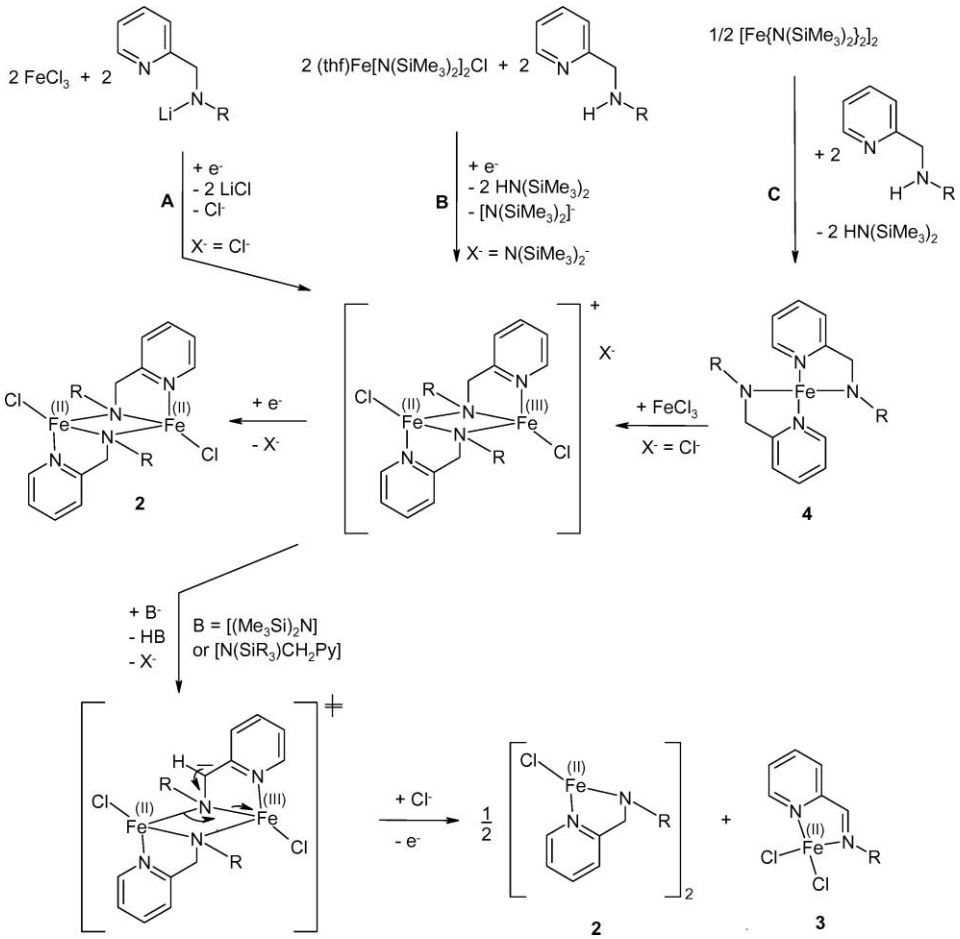

Scheme 2 Proposed mechanism for the synthesis of **2** and **3** *via* the oxidation of 2-pyridylmethylamides with iron(III).

Table 4 Comparison of selected bond lengths of iron complexes with terminally bound 2-Py-CH=NR ligands (L^{ox2}) and their reduced forms (see text and eqn (2))

Compound[a]	R	Type	Fe–N_{amide} (pm)	Fe–N_{Py} (pm)	NC/pm	Ref.
$[Cl_2Fe(Py'\text{-}CH{=}NR)]$	$cC_{12}H_{23}$	L^{ox2}	211.1	214.5	127.7	31
$[Cl_2Fe(Py\text{-}CH{=}NR)]$ (**3a**)	$SiMe_2tBu$	L^{ox2}	212.0	210.9	127.6	This work
$[Cl_2Fe(Py\text{-}CH{=}NR)]$ (**3b**)	$SiMe_2(CMe_2iPr)$	L^{ox2}	213.9	210.0	127.8	This work
$[Cl_2Fe(Py\text{-}CH{=}NR)]$ (**3c**)	$SiiPr_3$	L^{ox2}	213.0	210.9	127.5	This work
$[Cl_2Fe(Py\text{-}CH{=}NR)]$ (**3d**)[b]	$SiPh_3$	L^{ox2}	221.7	213.0	127.6	This work
$[Cl_2Fe(Py\text{-}CH{=}NR)]$[b]	$C_6H_3iPr_2$	L^{ox2}	222.7	215.0	127.2	31
$[Cl_2Fe(Py'\text{-}CH{=}NR)]$[b]	nPr	L^{ox2}	211.9	221.9	127.4	31
$[(thf)Fe(Py\text{-}CH{=}NR)_2]^+$	$C_6H_3iPr_2$	L^{ox1}/L^{ox2}	199.0	200.4	131.5	10
$[Fe(Py\text{-}CH{=}NR)_2]$	$C_6H_3iPr_2$	L^{ox1}	198.5	204.5	133.9	10
$[Fe(Py\text{-}CH_2\text{-}NR)_2]$ (**4a**)	$SiMe_2tBu$	HL	196.1	212.3	145.3	25
$[Fe(Py\text{-}CH_2\text{-}NR)_2]$ (**4d**)	$SiPh_3$	HL	196.7	211.2	145.6	This work

[a] Py = 2-pyridyl, Py′ = 6-methyl-2-pyridyl. [b] Compound is dimeric with bridging chloride anions.

in hexane (10.1 mmol). Then a solution of 3.0 g of chlorotriphenylsilane (10 mmol) was dropped at −78 °C into this mixture. After warming to r.t. and stirring for an additional 12 h, all volatile materials were removed under vacuum. The violet residue was dissolved in 15 ml of toluene and solids were removed by filtration. Removal of the solvent afforded 3.48 g of crystalline **1d** (9.48 mmol, 95%) which can be recrystallized from toluene. M.p. 93 °C. ^{1}H NMR ([D_6]benzene, δ (ppm)): 8.39 (d, $^3J(H_1H_2)$ = 4.4 Hz), 7.69–7.67 (m, 6H, *o*-Ph), 7.15–7.10 (m, 9H, *m*-Ph, *p*-Ph), 6.94 (td, $^3J(H_3H_{2/4})$ = 8 Hz, $^4J(H_3H_1)$ = 4.0 Hz, 1H, Py3), 6.70 (d, $^3J(H_4H_3)$ = 7.6 Hz, 1H, Py4) 6.54 (dd, $^3J(H_2H_{1/3})$ = 6.8 Hz and 7.2 Hz, 1H, Py2), 4.22 (d, ^3J(CHNH) = 7.2 Hz, 2H, C**H**$_2$), 2.53 (s, br., 1H, N**H**). ^{13}C{^{1}H}NMR ([D_6]benzene, δ (ppm)): 161.8 (Py5), 149.2 (Py1), 136.2 (Py3), 136.0 (*o*-Ph), 129.8 (*p*-Ph), 128.0 (m-Ph), 121.1 (Py2), 119.2 (Py4), 48.2 (**C**H$_2$). IR (Nujol, KBr, ν/cm^{-1}: 3370 s, 3063 s, 2666 w, 1957 w, br., 1892 w, br., 1827 w,

br., 1585 s, 1568 m, 1471 s, 1426 vs, 1402 s, 1308 w, 1276 w, 1203 w, 1180 w, 1143 m, 1113 vs, 1085 s, 1064 w, 1046 w, 1029 w, 994 m, 894 w, 843 s, 819 s, 763 s, 747 s, 738 s, 706 vs, 674 w, 620 w, 596 m, 523 s, 504 vs, 492 s, 455 m. MS (DEI, *m/z*): 365 (M^+, 2%), 290 ([Py-CH_2-NH-SiH_2Ph + H]$^+$, 98%), 259 ([$SiPh_3$]$^+$, 100%), 211([Py-CH_2-NH-SiH_2Ph + H]$^+$, 34%), 181 ([Py-CH-NPh − H]$^+$, 30%), 108 ([Py-CH_2-NH_2]$^+$, 7%). Elemental analysis ($C_{24}H_{21}N_2Si$, 366.53): calc.: C 78.64, H 6.05, N 7.64; found: C 77.82, H 5.95, N 7.60.

Chloro-(2-pyridylmethyl)(*tert*-butyldimethylsilyl)amidoiron(II) (2a) and dichloro-(2-pyridylmethylidene)(*tert*-butyldimethylsilyl)-aminoiron(II) (3a)

Method A. A solution of 0.20 g of (2-pyridylmethyl)(*tert*-butyldimethylsilyl)amine **1a** (0.97 mmol) in 5 ml of THF was dropped at r.t. to a solution of 0.47 g of (thf)Fe{$N(SiMe_3)_2$}$_2$Cl (0.97 mmol) in 15 ml of THF. After stirring for one day the volume of the green-brown solution was reduced to half of the original volume. After filtration 0.13 g of pale yellow cuboids of **2a** (0.21 mmol, 43%) precipitated at r.t. the crystals were washed with a small amount of THF. After slight reduction of the volume of the mother liquor another crop of crystals were collected. Now the volume of the residue was strongly reduced and 0.01 g of red platelets of **3a** (0.03 mmol, 3%) were collected.

Method B. (2-Pyridylmethyl)(*tert*-butyldimethylsilyl)amine (0.4 g, 1.8 mmol) in 5 ml of THF was lithiated at −78 °C with 1.1 ml of *n*-butyl lithium solution in hexane (1.6 M, 1.8 mmol). This solution was added dropwise at −78 °C to a solution of 0.15 g of $FeCl_3$ (0.9 mmol) in 5 ml of THF. After warming to r.t. and stirring for an additional 20 h, the solution was filtered. The volume of the filtrate was reduced to half of the original volume. At r.t. 0.05 g thin pale yellow needles of **2a** (0.08 mmol, 17%) precipitated within several days.

Data of 2a. M.p. 179 °C (dec.). IR (Nujol, KBr, ν/cm^{-1}: 1608 m, 1568 w, 1437 m, 1487 m, 1286 w, 1255 m, 1155 m, 1104 w, 1026 m, 991 m, 965 w, 899 w, 823 s br., 780 vs, 754 w, 709 w, 660 m, 638 w, 525 m, 467 w. MS (DEI, *m/z*): 625 (M^+, 1%), 567 ([M − *t*Bu]$^+$, 1%), 498 ([M − $FeCl_2$]$^+$, 4%), 441 ([M − $FeCl_2$ − *t*Bu]$^+$, 9%), 165 ([ampSiMe_2]$^+$, 100%). Elemental analysis ($C_{24}H_{42}Cl_2Fe_2Si_2N_4$; 625.71): calc.: C 46.07, H 6.77, N 8.95; found: C 45.43, H 6.59, N 8.81. Magnetism: μ_{eff} = 5.25 μ_B, 300 K.

Data of 3a. IR (Nujol, KBr, ν/cm^{-1}: 1622 m, 1593 s, 1568 w, 1298 m, 1255 m, 1222 m, 1156 w, 1102 w, 1020 m, 889 m, 840 s, 777 s, 681 w, 646 w. MS (DEI, *m/z*): 346 ([M]$^+$, 5%), 311 ([M − Cl]$^+$, 11%), 221 ([Py-CH=NSiMe_2*t*Bu]$^+$, 32%), 205 ([Py-CH=NSiMe*t*Bu]$^+$, 72%), 164 ([Py-CH=NSiMe_2]$^+$, 98%), 149 ([Py-CH=NSiMe_2]$^+$, 72%), 136 ([Py-CH=NSiMeH_2]$^+$, 85%), 106 ([Py-CH=NH]$^+$, 82%), 79 ([Py]$^+$, 100%). Elemental analysis ($C_{12}H_{20}Cl_2FeSiN_2$, 347.14): calc.: C 41.52, H 5.81, N 8.07; found: C 40.69, H 5.40, N 7.63. Magnetism: μ_{eff} = 5.1 μ_B, 300 K.

Chloro-(2-pyridylmethyl)(1,1,2-trimethylpropyl-dimethylsilyl)-amidoiron(II) (2b) and dichloro-(2-pyridylmethylidene)(1,1,2-trimethylpropyl-dimethylsilyl)aminoiron(II) (3b)

Method A. A solution of 0.27 g of (2-pyridylmethyl)(1,1,2-trimethylpropyl-dimethylsilyl)amine **1b** (1.10 mmol) in 10 ml of THF was dropped at r.t. into a solution of 0.52 g of (thf)Fe{$N(SiMe_3)_2$}Cl (1.10 mmol) in 10 ml of THF. After stirring for one day, the volume of the solution was reduced to a third of the original volume. At r.t. yellow platelets and brown needles crystallized. These crystals (0.07 g, 0.10 mmol, 17%) were isolated and X-ray diffraction studies showed that these crystals consisted of **2b** in the same space group. These crystals were washed with a few millilitres of THF and dried *in vacuo*. The mother liquor was concentrated to a few millilitres and then 0.04 g of orange-red needles of **3b** (0.11 mmol, 10%) precipitated within a few days.

Method B. (2-Pyridylmethyl)(1,1,2-trimethylpropyl-dimethylsilyl)amine **1b** (0.37 g, 1.5 mmol), dissolved in 5 ml of THF, was deprotonated with 1 ml of a 1.6 M solution of *n*BuLi in hexane (1.6 mmol) at −78 °C. This solution was dropped to a suspension of 0.24 g of $FeCl_3$ (1.5 mmol) in 5 ml of THF at −78 °C. Then the reaction mixture was warmed to −20 °C and stirred for two hours. Thereafter all solids were removed and the volume of the filtrate reduced to a few millilitres. Storage at −20 °C afforded the crystallization of 0.03 g of orange-red needles of **3b** (0.08 mmol, 6%). If the reaction mixture was warmed to r.t. during this procedure, the yield was even lower.

Data of 2b. M.p. 166 °C (dec.). IR (Nujol, KBr, ν/cm^{-1}: 1606 m, 1570 w, 1438 s, 1278 w, 1250 m, 1161 w, 1027 s, 993 w, 813 s, 775 vs, 744 w, 705 w, 659 w, 637 w, 528 w. MS (DEI, *m/z*): 680 (M^+, 0,3%), 595 ([M − *t*Hex]$^+$, 0.9%), 554 ([M − $FeCl_2$]$^+$, 4.6%), 469 ([M − $FeCl_2$ − *t*Hex]$^+$, 9.7%), 165 ([ampSiMe_2]$^+$, 100%). Elemental analysis ($C_{28}H_{50}N_4Cl_2Fe_2Si_2$, 681.49): calc.: C 49.35, H 7.40, N 8.22; found: C 47.54, H 7.32, N 7.85.

Data of 3b. M.p. 270 °C. IR (Nujol, KBr plates, ν/cm^{-1}: 1617 w, 1590 m, 1297 m, 1259 s, 1222 w, 1155 w, 1099 m, br., 1021 m, br., 891 m, 822 s, br., 789 m, 771 m, 723 w, 672 w. MS (DEI, *m/z*): 374 (M^+, 1.1%), 339 ([M − Cl]$^+$, 2%), 289 ([M − *t*Hex]$^+$, 1.8%), 254 ([M − *t*Hex − Cl]$^+$, 1.5%), 233 ([Py-CH=N-SiMe_2*t*Hex − Me]$^+$, 5,5%), 165 ([Py-CH_2-N=SiMe_2]$^+$, 100%). Elemental analysis ($C_{14}H_{24}N_2Cl_2FeSi$, 375.24): calc.: C 44.81, H 6.46, N 7.47; found: C 43.73, H 6.35, N 7.11. Magnetism: μ_{eff} = 5.2 μ_B, 300 K.

Chloro-(2-pyridylmethyl)(triisopropylsilyl)amidoiron(II) (2c) and dichloro-(2-pyridylmethylidene)(triisopropylsilyl)aminoiron(II) (3c)

Method A. A solution of 0.34 g of (2-pyridylmethyl)-(triisopropylsilyl)amine **1c** (1.29 mmol) in 20 ml of THF was added to a solution of 0.63 g of (thf)Fe{$N(SiMe_3)_2$}Cl (1.29 mmol) in 10 ml of THF. After reduction of the volume of the reaction mixture to half of the original volume and during storage at −20 °C, 0.07 g of pale yellow cuboids of **2c** (0.10 mmol, 16%) precipitated. Another crop of crystals were obtained after a repetition of this procedure. The crystals were washed with THF and dried under vacuum. The volume of the filtrate was strongly reduced and now, 0.09 g of violet platelets of **3c** (0.23 mmol, 18%) crystallized.

Method B. The reaction of 0.8 ml of 1.6 M *n*-butyl lithium solution in hexane with 0.34 g of (2-pyridylmethyl)-(triisopropylsilyl)amine (1.29 mmol) in 5 ml of THF at −78 °C gave the corresponding lithium amide which was added at −78 °C to a suspension of 0.21 g of $FeCl_3$ (1.3 mmol) in 5 ml of THF. Thereafter the reaction mixture was warmed to −20 °C and stirred

Table 5 Crystal data and refinement details for the X-ray structure determinations

Compound	**1d**	**2a**	**2b**	**2c**	**2d**	**3a**	**3b**	**3c**	**3d**	**4d**
Formula	$C_{24}H_{22}N_2Si$	$C_{24}H_{42}Cl_2Fe_2N_4Si_2\cdot C_6H_{14}$	$C_{28}H_{50}Cl_2Fe_2N_4Si_2$	$C_{30}H_{54}Cl_2Fe_2N_4Si_2$	$C_{48}H_{42}Cl_2Fe_2N_4Si_2\cdot 0.5\ C_4H_8O$	$C_{12}H_{20}Cl_2FeN_2Si$	$C_{14}H_{24}Cl_2FeN_2Si$	$C_{15}H_{26}Cl_2FeN_2Si$	$C_{48}H_{40}Cl_4Fe_2N_4Si_2$, $2(C_4H_8O)$	$C_{48}H_{42}FeN_4Si_2$
Fw/g mol^{-1}	366.53	711.57	681.50	709.55	949.69	347.14	375.19	389.22	1126.73	786.89
T/°C	–90(2)	–90(2)	–90(2)	–90(2)	–90(2)	–90(2)	–90(2)	–90(2)	–90(2)	–90(2)
Crystal system	Triclinic	Triclinic	Monoclinic	Triclinic	Monoclinic	Monoclinic	Triclinic	Monoclinic	Monoclinic	Orthorhombic
Space group	$P\bar{1}$	$P\bar{1}$	$P2_1/c$	$P\bar{1}$	$C2/c$	$P2_1/c$	$P\bar{1}$	$P2_1/c$	$P2_1/n$	$Fdd2$
a/Å	6.4898(3)	8.4163(7)	10.3393(5)	9.6409(4)	20.0652(8)	16.8690(9)	7.2991(5)	17.7619(15)	9.0029(4)	22.4134(8)
b/Å	10.3387(6)	10.9918(13)	11.7681(3)	11.7277(7)	14.6411(7)	13.2269(5)	8.0232(5)	7.6925(5)	18.7006(7)	37.3593(16)
c/Å	15.1982(8)	11.0332(12)	14.5255(7)	17.5459(9)	16.8566(6)	7.8214(5)	17.7411(13)	15.8045(13)	15.8978(4)	9.6921(5)
α/°	93.801(2)	112.081(5)	90	73.23(3)	90	90	81.560(5)	90	90	90.00
β/°	100.954(3)	99.969(6)	99.333(2)	88.47(3)	104.800(3)	100.908(3)	80.001(4)	112.645(3)	91.290(2)	90.00
γ/°	99.192(3)	94.411(6)	90	70.86(3)	90	90	64.211(4)	90	90	90.00
V/Å^3	983.38(9)	920.20(17)	1743.98(13)	1789.36(16)	4787.8(3)	1713.62(16)	918.29(11)	1992.9(3)	2675.87(17)	8115.7(6)
Z	2	1	2	2	4	4	2	4	2	8
ρ/g cm^{-3}	1.238	1.284	1.298	1.317	1.318	1.346	1.357	1.297	1.398	1.288
μ/cm^{-1}	1.3	10.23	10.77	10.52	8.07	12.48	11.7	10.81	8.32	4.7
Measured data	6965	6066	12 182	12 389	16 771	11 398	5715	12 798	17 985	14 135
Data with $I > 2\sigma(I)$	2950	2902	3025	5781	3358	2832	3280	3588	4170	3281
Unique data/R_{int}	4448/ 0.0371	4028/ 0.0319	3986/ 0.0463	8068/ 0.0311	5453/ 0.0730	3899/ 0.0497	3947/ 0.0268	4424/ 0.0358	6082/ 0.0601	4559/ 0.0796
wR_2 (all data, on F^2)[a]	0.1272	0.1018	0.0977	0.1125	0.1800	0.1171	0.1182	0.1048	0.1155	0.0851
R_1 ($I > 2\sigma(I)$)[a]	0.0513	0.0431	0.0373	0.0448	0.0567	0.0473	0.0444	0.0372	0.0454	0.0428
s[b]	1.013	1.007	1.013	0.996	1.019	1.013	1.002	1.074	1.008	0.977
Res. dens./ e Å^{-3}	0.277/ –0.303	0.334/ –0.422	0.296/ –0.375	0.814/ –0.437	0.894/ –0.450	0.593/ –0.374	0.918/ –0.776	0.364/ –0.384	0.555/ –0.431	0.271/ –0.232
CCDC No.	676619	676620	676621	676622	676623	676624	676625	676626	736365	736366

[a] Definition of the R indices: $R_1 = (\sum\|F_o| - |F_c\|)/\sum|F_o|$ w$R_2 = \{\sum[w(F_o^2 - F_c^2)^2]/\sum[w(F_o^2)^2]\}^{1/2}$ with $w^{-1} = \sigma^2(F_o^2) + (aP)^2$. [b] $s = \{\sum[w(F_o^2 - F_c^2)^2]/(N_o - N_p)\}^{1/2}$.

for an additional 2.5 h. Then the solution was filtered at –20 °C and the volume was reduced under reduced pressure also at this temperature. Storage at –20 °C leads to the precipitation of 0.06 g of violet needles of **3c** (0.15 mmol, 12%). Warming of the reaction mixture to r.t. led to yields of less than 5%.

Data of 2c. M.p. 179 °C (dec.), IR (Nujol, KBr, ν/cm^{-1}: 1605 m, 1570 m, 1480 m, 1437 s, 1281 m, 1249 w, 1153 w, 1105 w, 1051 w, 1026 m, 1001 m, 976 m, 917 w, 882 m, 822 w, 771 vs, 751 s, 707 m, 666 m, 650 m, 510 m, 471 m. MS (DEI, m/z): 709 (M^+, 0.04%), 666 ([M – *i*Pr]$^+$, 0.1%), 582 ([M – $FeCl_2$]$^+$, 0.8%), 539 ([M – $FeCl_2$ – *i*Pr]$^+$, 1%), 264 ([ampSi^{i}Pr$_3$]$^+$, 6%), 220 ([ampSi^{i}Pr$_2$ – H]$^+$, 100%), 135 ([ampSi – H]$^+$, 90%). Elemental analysis ($C_{30}H_{54}N_4Cl_2Fe_2Si_2$; 709.54): calc.: C 50.78, H 7.67, N 7.90; found: C 49.36, H 7.67, N 7.64.

Data of 3c. M.p. 226 °C. IR (Nujol, KBr, ν/cm^{-1}: 1615 m, 1591 s, 1566 w, 1300 m, 1221 w, 1102 w, 1020 m, 883 s, 789 m, 776 m, 692 m, 655 w, 623 w, 508 w, 489 w. MS (DEI, m/z): 388 (M^+, 40%), 353 ([M – Cl]$^+$, 98%), 345 ([M – *i*Pr]$^+$, 28%), 310 ([M – *i*Pr – Cl]$^+$, 45%), 261 ([Py-CH=NSi(^{i}Pr)$_3$]$^+$, 13%), 218 ([Py-CH=NSi(^{i}Pr)$_2$]$^+$, 100%), 176 ([Py-CH=NSi ^{i}Pr]$^+$, 16%), 133 ([Py-CH=NSi]$^+$, 88%) 106 ([Py-CH=NH]$^+$, 71%). Elemental analysis ($C_{15}H_{26}N_2Cl_2FeSi$; 389,22): calc.: C 46.29, H 6.73, N 7.20; found: C 44.57, H 6.43, N 7.40. Magnetism: $\mu_{eff} = 4.9\ \mu_B$, 300 K.

Chloro-(2-pyridylmethyl)(triphenylsilyl)amidoiron(II) (2d) and dimeric dichloro-(2-pyridylmethylidene)(triphenylsilyl)amino-iron(II) (3d)

Method A. A solution of 0.27 g of (2-pyridylmethyl)(triphenylsilyl)amine (0.73 mmol) in 10 ml of THF was added to a solution of 0.37 g of (thf)Fe{N(SiMe$_3$)$_2$}Cl (0.75 mmol) in 10 ml of THF. After stirring for one day, the volume of the reaction mixture was reduced to half of the original volume. After filtration the filtrate was stored at r.t. Within two days 0.12 g of pale yellow platelets of **2d** (1.3 mmol, 36%) precipitated and were dried *in vacuo*. After reduction of the volume of the mother liquor blue needles of **3d** were obtained, however, this compound always contained varying amounts of **2d**. Therefore, only an X-ray structure determination of **3d** was performed in order to proof the constitution of this complex.

Method B. A solution of 0.66 g of {Fe[N(SiMe$_3$)$_2$]$_2$}$_2$ (0.88 mmol) in 5 ml of THF was added to a solution of 0.60 g (2-pyridylmethyl)(triphenylsilyl)amine (1.63 mmol) in 5 ml of THF. After stirring at r.t. for 30 min all solids were removed by filtration. The filtrate was layered with 5 ml of THF and then with a solution of 0.26 g of iron(III)chloride (1.63 mmol) in 5 ml of THF. Diffusion at r.t. led to crystallization of **2d** and **3d** in the shape of dark blue needles and also of $Fe_4Cl_8(thf)_6$ in the shape of colorless cuboids.

Separation and purification of **3d** failed, the impurities consisted of **2d** and $Fe_4Cl_8(thf)_6$.

Physical data of 2d. M.p. 120 °C. IR (Nujol, KBr windows, ν/cm^{-1}: 3065 m, 3042 m, 2683 br. w, 1976 br. w, 1906 br. w, 1831 br. w., 1605 s, 1587 m, 1570 m, 1483 s, 1440 s, 1426 s, 1281 m, 1259 m, 1259 m, 1188 w, 1161 m, 1110 br. s, 1068 m, 1026 s, 988 m, 911 w, 889 w, 820 w, 781 vs, 748 s, 710 vs, 670 w, 650 m, 636 s, 550 vs, 516 vs, 495 s, 485 m, 459 w. MS (DEI, m/z): 356 ([amp-$SiPh_3$]$^+$, 4%), 289 ([amp-$SiPh_2$]$^+$, 100%), 259 ([$SiPh_3$]$^+$, 97%), 181 ([$SiPh_2$]$^+$, 59%), 105 ([SiPh]$^+$, 40%), 78 ([Ph + H]$^+$, 20%). Elemental analysis ($C_{48}H_{42}N_4Si_2Fe_2Cl_2$, 913.64): calc.: C 63.10, H 4.63, N 6.13; found: C 62.90, H 5.26, N 5.79.

Data of 3d. MS (DIE, m/z): 492 (M^+, > 1%), 456 ([M – Cl]$^+$, > 1%), 364 ([Py-CH=N$SiPh_3$]$^+$, 2%).

Iron(II) bis[(2-pyridylmethyl)(triphenylsilyl)amide] (4d)

A solution of 0.47 g of $\{Fe[N(SiMe_3)_2]_2\}_2$ (0.63 mmol) in 5 ml of toluene was added to a solution of 0.46 g of (2-pyridylmethyl)(triphenylsilyl)amine (1.25 mmol) in 5 ml of toluene. After stirring for 30 min all solid materials were removed by filtration. Thereafter the solvent was removed in vacuum and the green residue was dried under reduced pressure. After dissolving in diethyl ether orange crystals precipitated at r.t. which were washed with small portions of ether and dried *in vacuo*. Yield: 0.35 g (0.44 mmol, 70%). M.p. 195 °C. IR (Nujol, KBr windows, ν/cm^{-1}: 3043 m (sh), 2013 w, 1952 w, 1880 w, 1826 w, 1765 w, 1713 w, 1598 m, 1562 m, 1341 m, 1302 m, 1276 m, 1186 w, 1150 m, 1113 m (br)., 1045 m, 977 m, 952 m, 887 m (br)., 806 m, 737 s (br)., 700 s (br)., 609 m, 563 m, 500 m (br). MS (DIE, m/z): 786 (M^+, 5%), 709 ([M – Ph]$^+$, 1%), 631 ([M – 2Ph]$^+$, 1%], 420 ([M – Py – CH_2 – $NHSiPh_3$]$^+$, 5%], 289 ([Py – CH_2 – $NHSiPh_2$]$^+$, 100%]. Elemental analysis ($C_{48}H_{42}N_4FeSi_2$, 786.89): calc.: C: 73.26, H 5.28, N 7.12, found: C 72.76, H 5.44, N 6.89. Magnetism: $\mu_{eff} = 6.3\ \mu_B$, 300 K.

X-Ray structure determinations

The intensity data for the compounds were collected on a Nonius KappaCCD diffractometer using graphite-monochromated Mo-Kα radiation. Data were corrected for Lorentz and polarization effects but not for absorption effects.[33,34] Crystal data and refinement details for the X-ray structure determinations are summarized in Table 5.

The structures were solved by direct methods (SHELXS)[35] and refined by full-matrix least squares techniques against F_o^2 (SHELXL-97).[36] For the amine-group at N1 of **1d** and for the methylene-group at C6 at **2a** the hydrogen atoms were located by difference Fourier synthesis and refined isotropically. The other hydrogen atoms were included at calculated positions with fixed thermal parameters. All non-disordered, non-hydrogen atoms were refined anisotropically.[36] XP (SIEMENS Analytical X-ray Instruments, Inc.) was used for structure representations.

Acknowledgements

This work was supported by the *Deutsche Forschungsgemeinschaft* (DFG, Bonn-Bad Godesberg, Germany). We also acknowledge the support by the *Fonds der Chemischen Industrie* (Frankfurt/Main, Germany). A. Malassa thanks the Carl-Zeiss-Stiftung (Germany) for a generous Ph.D. grant.

References

1 D. M. Roundhill, *Chem. Rev.*, 1992, **92**, 1–27.
2 R. H. Holm, P. Kennepohl and E. I. Solomon, *Chem. Rev.*, 1996, **96**, 2239–2314.
3 (*a*) W. Kaim and B. Schwederski, *Bioinorganic Chemistry: Inorganic Elements in the Chemistry of Life*, Wiley, Chichester, 1994; (*b*) J. J. R. Fraústo da Silva and R. J. P. Williams, *The Biological Chemistry of the Elements*, 2nd edn, Oxford University Press, Oxford, 2001.
4 T. A. Jackson, L. Que, H.-B. Kraatz and N. Metzler-Nolte, *Concepts and Models in Bioinorganic Chemistry*, Wiley-VCH, Weinheim, 2006, pp. 259–286.
5 K. Chen, M. Costas and L. Que, *J. Chem. Soc., Dalton Trans.*, 2002, 672–679.
6 A. L. Gavrilova and B. Bosnich, *Chem. Rev.*, 2004, **104**, 349–383.
7 M. Costas, M. P. Mehn, M. P. Jensen and L. Que, *Chem. Rev.*, 2004, **104**, 939–986.
8 X. Shan and L. Que, *J. Inorg. Biochem.*, 2006, **100**, 421–433.
9 M. Ostermeier, C. Limberg, B. Ziemer and V. Karunakaran, *Angew. Chem.*, 2007, **119**, 5423–5426; M. Ostermeier, C. Limberg, B. Ziemer and V. Karunakaran, *Angew. Chem., Int. Ed.*, 2007, **46**, 5329–5331.
10 C. C. Lu, E. Bill, T. Weyhermüller, E. Bothe and K. Wieghardt, *J. Am. Chem. Soc.*, 2008, **130**, 3181–3197.
11 (*a*) J. T. B. H. Jastrzebski, J. M. Klerks, G. van Koten and K. Vrieze, *J. Organomet. Chem.*, 1981, **210**, C49–C53; (*b*) G. van Koten, J. T. B. H. Jastrzebski and K. Vrieze, *J. Organomet. Chem.*, 1983, **250**, 49–61; (*c*) E. Wissing, S. von der Linden, E. Rijnberg, J. Boersma, W. J. J. Smeets, A. L. Spek and G. van Koten, *Organometallics*, 1994, **13**, 2602–2608.
12 M. Westerhausen, A. N. Kneifel and N. Makropoulos, *Inorg. Chem. Commun.*, 2004, **7**, 990–993.
13 M. Westerhausen, T. Bollwein, N. Makropoulos, S. Schneiderbauer, M. Suter, H. Nöth, P. Mayer, H. Piotrowski, K. Polborn and A. Pfitzner, *Eur. J. Inorg. Chem.*, 2002, 389–404.
14 M. Westerhausen, A. N. Kneifel and P. Mayer, *Z. Anorg. Allg. Chem.*, 2006, **632**, 634–638.
15 M. Westerhausen, T. Bollwein, N. Makropoulos, T. M. Rotter, T. Habereder, M. Suter and H. Nöth, *Eur. J. Inorg. Chem.*, 2001, 851–857.
16 Y. Okamoto, K. Ogura and T. Kinoshita, *Polyhedron*, 1984, **3**, 635–638.
17 K. Ogura, Y. Kurasawa, Y. Yamaguchi and Y. Okamoto, *Heterocycles*, 2003, **59**, 283–291.
18 C. J. Davies, G. A. Solan and J. Fawcett, *Polyhedron*, 2004, **23**, 3105–3114.
19 G. Chen, Y.-X. Sun, M. Sun and W. Qi, *Acta Crystallogr., Sect. E: Struct. Rep. Online*, 2004, **60**, m1547–m1549.
20 K. W. Törnroos, D. Chernyshov, M. Hostettler and H.-B. Bürgi, *Acta Crystallogr., Sect. C: Cryst. Struct. Commun.*, 2005, **61**, m450–m452.
21 A. Malassa, H. Görls, A. Buchholz, W. Plass and M. Westerhausen, *Z. Anorg. Allg. Chem.*, 2006, **632**, 2355–2362.
22 D. C. Bradley and M. H. Chisholm, *Acc. Chem. Res.*, 1976, **9**, 273–280.
23 M. F. Lappert, P. P. Power, A. R. Sanger and R. C. Srivastava, *Metal and Metalloid Amides: Syntheses, Structures, and Physical and Chemical Properties*, Ellis Horwood, Chichester, 1980, ch. 8, pp. 465–544.
24 M. Lappert, A. Protchenko, P. Power and A. Seeber, *Metal Amide Chemistry*, Wiley, Chichester 2009, ch. 6, pp. 149–204.
25 R. A. Andersen, K. Faegri, J. C. Green, A. Haaland, M. F. Lappert, W.-P. Leung and K. Rypdal, *Inorg. Chem.*, 1988, **27**, 1782–1786.
26 C. Koch, A. Malassa, C. Agthe, H. Görls, R. Biedermann, H. Krautscheid and M. Westerhausen, *Z. Anorg. Allg. Chem.*, 2007, **633**, 375–382.
27 D. C. Bradley, R. G. Copperthwaite, M. W. Extine, W. W. Reichert and M. H. Chisholm, *Inorg. Synth.*, 1978, **18**, 112–120.
28 J. S. Duncan, T. M. Nazif, A. K. Verma and S. C. Lee, *Inorg. Chem.*, 2003, **42**, 1211–1224.
29 J. Zeller, S. König and U. Radium, *Inorg. Chim. Acta*, 2004, **357**, 1813–1821.
30 H. Zhao, R. Clérac, J.-S. Sun, X. Ouyang, J. M. Clemente-Juan, C. J. Gómez-García, E. Coronado and K. R. Dunbar, *J. Solid State Chem.*, 2001, **159**, 281–292.

31 V. C. Gibson, R. K. O'Reilly, D. F. Wass, A. J. P. White and D. J. Williams, *Dalton Trans.*, 2003, 2824–2830.
32 See *e.g.* (*a*) J. E. Huheey, *Anorganische Chemie: Prinzipien von Struktur und Reaktivität*, 3rd edn, Harper & Row: New York, 1983, pp. 517–530; (*b*) M. Mohan, S. G. Mittal, H. C. Khera and A. K. Sirivastava, *Gazz. Chim. Ital.*, 1977, **107**, 393–397.
33 *COLLECT, Data Collection Software* Nonius B.V., Netherlands, 1998.
34 Processing of X-Ray Diffraction Data Collected in Oscillation Mode, Z. Otwinowski, W. Minor, in C. W. Carter, R. M. Sweet, ed.: *Methods in Enzymology, Vol. 276, Macromolecular Crystallography, Part A*, pp. 307–326, Academic Press, 1997.
35 G. M. Sheldrick, *Acta Crystallogr., Sect. A: Found. Crystallogr.*, 1990, **46**, 467–473.
36 G. M. Sheldrick, *SHELXL-97* (Release 97-2), University of Göttingen, Germany, 1997.

